356

Storm Prediction over Europe using the ECMWF Ensemble Prediction System

Roberto Buizza and
Anthony Hollingsworth

Research Department

January 2002
In press in Meteorological Applications

For additional copies please contact

The Library
ECMWF
Shinfield Park
Reading, Berks RG2 9AX

library@ecmwf.int

Series: ECMWF Technical Memoranda

A full list of ECMWF Publications can be found on our web site under:
http://www.ecmwf.int/pressroom/publications.html

Abstract

Three severe storms caused great damage in Europe in December 1999. The first storm hit Denmark and Germany on the 3rd and the 4th of December, and the other two storms crossed France and Germany on the 26th and the 28th of December.

Firstly, the performance of the Ensemble Prediction System (EPS) operational at the European Centre for Medium-Range Weather Forecast (ECMWF) in predicting these intense storms is investigated. Results indicate that the EPS gave early indications of possible severe storm occurrence, and was especially useful when the deterministic TL319L60 forecasts issued on successive days were highly inconsistent. These results indicate that the EPS is a valuable tool for assessing quantitatively the risk of severe weather and issuing early warnings of possible disruptions.

Secondly, the impact of an increase of the ensemble system horizontal resolution (T L255 integration from a TL511 analysis instead of the operational T L159 integration from a TL319 analysis) on the system performance is also investigated. Results show that the resolution increase enhances the ensemble performance in predicting the position and the intensity of intense storms.

1. INTRODUCTION

Human activities have become increasingly more vulnerable to severe weather (*Kunkel et al.* 1999, *Easterling et al.* 1999) and there is an increasing demand that numerical weather prediction centers provide reliable forecasts of such severe events. Early indications of severe weather events are necessary to improve the quality of systems designed to issue early warnings of potentially severe damages. In the United States, average costs of $16 billion are incurred annually for weather-related damages (*Pielke* 1997).

Severe events are often associated with very energetic phenomena such as flooding, strong winds and extreme temperatures. In forecasting such events small errors in the initial conditions may grow very quickly and affect the forecast accuracy. Furthermore, model uncertainties due to the discrete representation of the system equations may increase the forecast error growth. As a consequence, forecasting systems based on single deterministic forecasts may not be reliable.

Since 1992, ensemble prediction systems based on multiple integrations of model equations have become part of the operational numerical weather prediction practice (*Palmer et al.* 1993, *Toth & Kalnay* 1993, *Houtekamer et al.* 1996). Ensemble prediction provides a tool for quantifying the risk of severe weather.

At the European Centre for Medium-Range Weather Forecasts (ECMWF), the Ensemble Prediction System (*Molteni et al.* 1996) has been designed to simulate both initial and model uncertainties. The initial uncertainties are simulated by starting the multiple integrations from perturbed initial conditions (*Buizza & Palmer* 1995). Model uncertainties due to the parameterized physical processes are simulated by stochastically perturbing the model equations (*Buizza et al.* 1999).

Two main issues are discussed in this work. First, the performance of the ECMWF forecasting system during the three severe storms that caused great damage in Europe in December 1999 is discussed. At the time of the events, the deterministic high-resolution model had horizontal spectral triangular truncation T319 with

linear grid and 60 vertical levels (T_L319L60) and the EPS had resolution T_L159L40 and 51 members, with initial conditions defined from the T_L319L60 analysis. The first storm hit Denmark and Germany on the 3rd and the 4th of December, and the other two storms crossed France and Germany on the 26th and the 28th of December. Strong winds associated with intense fast-moving cyclones caused serious disruptions, several deaths and billion of dollars ($US) of damages (*Bell et al.* 2000). Numerous buildings and vast areas of forests were destroyed by the winds, while transport and power outages affected large areas for several days.

Then, the impact of an increase of the ensemble system horizontal resolution is investigated. EPS forecasts are compared with forecasts from a higher resolution experimental ensemble system (HEPS) based on 51 members as the EPS but with higher horizontal resolution (T_L159 instead of T_L255) and with initial conditions defined from a higher-resolution T_L511 analyses (by contrast, the EPS initial conditions were defined using operational T_L319 analyses). This high-resolution configuration became operational at ECMWF on the 21st of November 2000. The performance of the HEPS and the EPS are compared.

2. The ECMWF Ensemble Prediction System

Since December 1996, the ECMWF EPS has been based on 51 members at T_L159L31 resolution (spectral triangular truncation T159 with linear grid, *Buizza et al.* 1998). In October 1998, a scheme to simulate model uncertainties due to random model error in the parameterized physical processes was introduced (*Buizza et al.* 1999), and in October 1999 the number of vertical levels of the EPS was been increased to 40, with the extra levels in the planetary boundary layer (*Teixeira* 1999).

Schematically, the current EPS can be described as follows. Each EPS forecast e_j is generated by integrating the perturbed model equations

$$\frac{\partial e_j}{\partial t} = A(e_j,t) + P'_j(e_j,t) \tag{1}$$

starting from perturbed initial conditions

$$e_j(t=0) = e_0(t=0) + \delta e_j(t=0) \tag{2}$$

A and P' identify the contribution to the full equation tendency of the non-parameterized and parameterized physical processes. For each grid point $\boldsymbol{x}=(\lambda,\phi,\sigma)$ (identified by its latitude, longitude and vertical hybrid coordinate), the perturbed parameterized tendency P' (of each state vector component) is defined as

$$P'_j(e_j,t) = [1+ < r_j(\lambda,\phi,t) >_{D,T}]P(e_j,t) \tag{3}$$

where P is the unperturbed diabatic tendency, and $<..>_{D,T}$ indicates that the same random number r_j has been used for all grid points inside a DxD degree box and over T time steps. The random numbers are currently sampled uniformly in the interval *[-0.5,0.5]*, the same random number is used inside *10° degrees* boxes (*D=10*), and the set of random numbers is updated every *6 hours* (*T=6*) (note that random numbers do not vary with the vertical coordinate).

$e_0(t=0)$ in Equation (0 is the operational analysis at $t=0$, while δe_j denotes the j-th initial perturbation. For each initial day d, the initial perturbations are defined using the singular vectors growing in the forecast range between day d and day $d+2$ at initial time, and the singular vectors that had grown in the past between day $d-2$ and day d at final time

$$\delta e_j(t=0) = \sum_{i=1}^{25}[\alpha_{i,j} v_i^{d,d+2}(t=0) + \beta_{i,j} v_i^{d-2,d}(t=48h)] \quad (4)$$

where $\boldsymbol{v}_i^{d,d+2}(t=0)$ is the *i-th* singular vector growing between day d and $d+2$ at time $t=0$ (*Barkmeijer et al.* 1999). The coefficients $\alpha_{i,j}$ and $\beta_{i,j}$ set the initial amplitude of the ensemble perturbations, and are defined by comparing the singular vectors with estimates of analysis errors (*Molteni et al.* 1996).

At the time of the events under investigation the ensemble forecasts were post-processed and saved only every 12-hours (since March 2000 ensemble surface variables are post-processed and saved every 6 hours). As a consequence and since the initial time for the ECMWF operational ensemble is 12 UTC, verification can only be performed either at 00 or at 12 UTC.

3. Measures of forecast accuracy

Forecast verification is focused on mean-sea-level-pressure (MSLP), with forecasts started on subsequent days are verified at the same forecast time inside regions centered on the observed storms. The quality of the single deterministic and ensemble prediction is assessed by computing the error in the prediction of the intensity (Intensity Error, IE) and of the position (Position Error, PE) of the MSLP minimum value. Local minimum values are searched inside a verification region centered on the observed storm, and if found the position and the intensity of the MSLP minimum value is computed (this software was kindly provided by *Martin Leutbecher*). The intensity error IE (in hPa) is the absolute difference between the forecast and analysis pressure minimum and the position error PE is the distance (in km) between the forecast and the analyzed position. The root-mean-square error (RMSE) inside a verification area centered on the storm observed position is also computed, but the RMSE should be used with care when considering the prediction of fields characterized by a strong gradient such as deep lows. In this cases, in fact, a smooth forecast without any deep low could have a smaller RMSE than a forecast with a misplaced deep low, which maybe more informative than the previous one. The intensity and position error should be preferred in this case.

4. The Danish/German storm (3-4 December 1999)

This storm affected Denmark, Germany and other Baltic countries on the 3rd and the 4th of December 1999 (Fig. 1). A low-pressure system located northwest of Ireland at 00UTC on the 3rd of December (Fig. 1a) deepened from 996hPa to 961hPa during the following 12 hours (Fig. 1b) while moving eastward. In the next 12 hours the cyclone continued eastward into the Baltic sea while MSLP dropped from 961hPa to 957hPa (Fig. 1c), and then continued to move eastward while weakening its intensity (Fig. 1d). Since forecasts issued at short forecast ranges (say up to t+72h) were rather accurate (see discussion below), attention will be focused mainly on the t+132h and the t+84h forecast ranges.

Forecasts are verified at 00UTC on the 4th of December when the cyclone reached its strongest intensity and was located northeast of Denmark (Fig. 1c). The verification area used to compute the RMSEs has longitude between 0 and 25˚E and latitude between 48˚N and 62˚N. Consideration of other verification times would have led to qualitatively similar conclusions.

4.1 Performance of the ECMWF deterministic T_L319L60 model

Table 1a lists the IE/PE errors of the T_L319L60 forecasts issued from the 26th of November (t+180h) to the 2nd of December (t+36h). Figure 2 shows the analysis of 00UTC on the 4th of December and the deterministic T_L319L60 forecast started on the 28th of November (t+132h). Figure 3 shows the corresponding forecasts started on the 30th of November (t+84h). The T_L319L60 forecasts issued between the 26th (t+180h) and the 30th (t+84h) of November were very inconsistent, with forecasts with low IE/PE alternated by forecasts with large errors (Table 1a). Only the T_L319L60 forecasts issued on the 1st (t+60h) and 2nd (t+36h) of December had IE/PE smaller than 10hPa/300km.

4.2 Performance of the operational and of the high-resolution EPS

The EPS control performed similarly to the T_L319L60 for forecast ranges longer than 60 hours while the T_L319L60 forecast performed better for shorter forecast times. The ensemble-mean, which is the most immediate product that can be constructed using the EPS, had an RMSE higher than the EPS control forecast for all forecast ranges (not shown). This should not surprise since the ensemble-mean, even if it is a smoother field than any single forecasts, cannot be expected to have a smaller RMSE when only one single case of a prediction of a deep low is considered. Table 1a lists the intensity and position errors of the EPS control and the T_L319L60 forecasts.

The EPS started on the 26th and the 27th of November (t+180h and t+156h, not shown) had only one member predicting the storm with IE<10hPa and 300km<PE<600km. Figure 2 shows the EPS control, the ensemble-mean and five selected EPS members started on the 28th of November (t+132h). The selected members are the two EPS members with the smallest RMSE and the three members with the smallest IE. Figure 2 shows that the ensemble-mean forecast did not provide any indication of the possibility of a storm affecting the verification area. Figure 3 shows the EPS control, the ensemble-mean and five EPS selected members issued of the 30th of November (t+84h). These forecasts were more accurate than the forecasts issued two days before (Fig. 2), with fifteen EPS members characterized by IE/PE smaller than 20hPa/600km (Table 2, top-left gray-shaded area). Again, note that the ensemble-mean forecast did not give any indication of the possibility of a storm affecting the verification area.

Figure 4 shows the high-resolution ensemble (HEPS) t+132h forecasts corresponding to the EPS forecasts shown in Fig. 2. Compared to the EPS (Fig. 2), the HEPS forecasts predicted more correctly both the storm intensity and its position. HEPS member 2, which had the lowest RMSE of all forecasts (3.0hPa), had intensity/position errors of 5hPa/120km. HEPS member 3, ranked in second position according to RMSE (7.2hPa) and characterized by the smallest IE, had intensity/position errors of 0.4hPa/207km (for this forecast range, the T_L319L60 forecast had an RMSE of 7.6hPa and intensity/position errors of 13.1hPa/149km). Figure 5 shows the t+84h HEPS forecasts. The t+84h HEPS forecasts had much smaller intensity errors than the corresponding EPS forecasts (Fig. 3). This is summarized in Table 2, which lists the

impact the horizontal resolution increase on the IE/PE of the t+132h and the t+84h forecasts. The HEPS not only had a larger number of good forecasts (top-left gray-shaded area in Tables 2a,b) but it also had a lower number of poor forecasts (bottom-right gray-shaded area in Tables 1a,b), especially for the t+84h forecast range.

Figure 6 shows some IE/PE and the RMSE statistics of the EPS and HEPS. Results indicate that the number of EPS and HEPS members with small errors had been consistently increasing during subsequent days while approaching the verification time, and that the HEPS forecasts had smaller intensity and position errors, especially at short forecast ranges (t+36h and t+60h).

5. The French/German storms (26-28 December 1999)

During the days after Christmas 1999 Western Europe was hit by a sequence of intense storms. The first storm crossed French in the early hours of the 26th of December (Fig. 7a,b), causing severe damage. The second storm hit southwestern France on the 27th of December and the alpine region on the 28th of December (Fig. 7d-f). These two storms originated in the western Atlantic and moved very rapidly eastward in the very strong zonal flow. The two storms were very different in scale: while the first storm was a very small-scale vortex moving extremely rapidly (it crossed France in less than 12 hours), a larger scale characterized the second storm.

The atmospheric flow during this period was very complex, with small-scale vortices developing and interacting while moving very rapidly in the strong zonal flow. At one time, three of these intense vortices were positioned very closely, affecting France, the UK and the Eastern Atlantic. The fact that the flow was difficult to predict is confirmed by the strong inconsistency of $T_L319L60$ forecasts issued on successive days. Since long and medium range forecasts were rather poor up to t+60h especially for the first storm (see discussion below), verification will focus on the t+48h forecast range for the first storm and the t+60h forecast range for the second storm.

Forecasts for the first storm are verified at 12UTC on the 26th of December (Fig. 7b) and forecasts for the second storm are verified at 00UTC on the 28th of December (Fig. 7e). Two different verification areas are used to compute the RMSE at the two verification times, each of them centered on the observed position. The first area has longitude between 5˚W and 20˚E and latitude between 40˚N and 57˚N, while the second area has longitude between 10˚W and 20˚E and latitude between 40˚N and 57˚N. Verification at other times would have drawn qualitatively similar conclusions.

5.1 Performance of the ECMWF deterministic $T_L319L60$ model

5.1.1 First storm (verification time 12UTC on the 26th of December)

The top two panels of Fig. 8 shows the analysis and the $T_L319L60$ forecast issued the 24th of December (t+48h). At the 48h forecast range, the $T_L319L60$ forecast almost correctly positioned the large-scale trough but failed to predict the storm intensity and position. Table 1b lists the IE/PE of the $T_L319L60$ forecast issued from the 19th (t+168h) to the 25th (t+24h) of December. The $T_L319L60$ forecasts issued on the 19th (t+168h) and on the 20th of December (t+144h) were rather accurate in describing the large-scale flow and had an RMSE of about 8hPa, but had very large IE/PE (Table 1b). The $T_L319L60$ forecast issued on the 21st

of December (t+120h) wrongly predicted a zonal flow instead of the deep trough. The T_L319L60 forecasts issued the following days were very inconsistent, with forecasts with either large IE or large PE (the t+96h issued the 22nd and the t+48h issued the 24th) alternated by more accurate forecasts (the t+72h issued the 23rd and the t+24h issued the 25th).

5.1.2 Second storm (verification time 00UTC on the 28th of December)

The top two panels of Fig. 9 shows the analysis and the T_L319L60 forecast issued the 25th of December (t+60h). At this forecast range, the T_L319L60 forecast missed the prediction of the storm. Table 1c lists the IE/PE of the T_L319L60 forecast issued from the 20th (t+180h) to the 26th (t+36h) of December. Table 1c indicates that the T_L319L60 forecast issued the 21st of December (t+156h) was the only forecast with small IE/PE (4.3hPa/169km), preceded and followed by forecasts characterized by large IE/PE (Table 1c).

5.2 Performance of the operational and the high-resolution EPS

5.2.1 First storm (verification time 12UTC on the 26th of December)

The EPS control performed similarly to the T_L319L60 forecast (the T_L319L60 was better than the EPS control at the 168h and 96h forecast ranges, while the EPS control was better for the other forecast ranges). Table 1b shows that in terms of IE/PE the EPS control was worse than the T_L319L60 forecast for forecast ranges up to 96h, but it was better for shorter forecast ranges.

Figure 8 shows the EPS control, the ensemble-mean and five selected EPS forecasts started on the 24th of December (t+48h). Eleven EPS members had an RMSE smaller than the T_L319L60 forecast and six EPS members had intensity/position errors smaller than 10hPa/600km. Figure 10 shows the corresponding HEPS t+48h forecasts. Compared to the EPS (Fig. 8), the HEPS members were better able to predict the small-scale vortex. HEPS member 49 had the lowest RMSE (2.7hPa) and HEPS member 44 had the lowest IE (0.2hPa) of all forecasts.

Figure 11a shows some IE/PE statistics for all forecast issued from the 19th (t+168h) to the 25th (t+24h) of December. None of the EPS members predicted the storm with IE/PE smaller than 10hPa/300km and at most 9 members predicted the storm with IE/PE smaller than 20hPa/600km. Figure 11a shows that for all forecast ranges, HEPS forecasts were characterized by smaller IE/PE. Figure 11b shows RMSE statistics for both the EPS and the HEPS forecasts. Only up to two EPS members had a RMSE smaller than 5hPa up to the 96h forecast range, while this number steadily increased for shorter forecast ranges. Figure 11b shows that the HEPS had more members than the EPS with an RMSE smaller than 10hPa but has less members with RMSE smaller than 5hPa.

Table 3 highlights in more details the impact of horizontal resolution on the 120h and 48h forecasts. At both these forecast ranges, the HEPS had more forecasts with IE/PE smaller than 10hPa/300km (three compare to zero at t+132h and one compared to zero at t+60h), but the HEPS has also more members with large errors.

5.2.2 Second storm (verification time 00UTC on the 28th of December)

The EPS control performed on average again similarly to the T_L319L60 forecast. In terms of IE/PE (Table 1c) the T_L319L60 forecast and the EPS control had comparable errors for all but the t+156 forecast range, for which the T_L319L60 forecast was more accurate.

Figure 9 shows the EPS control, the ensemble-mean and five selected EPS members started on the 25th of December (t+60h). Twenty-eight EPS members had an RMSE smaller than the T_L319L60 model, and thirty-six had an IE smaller than the T_L319L60 model. EPS member 1, best in terms of RMSE, had IE=3.8hPa and PE=138km. The two EPS members with the lowest IE, members 11 and 35, are ranked in 45th and 14th position according to RMSE. EPS members 34, ranked in 2nd position according to RMSE, is ranked in 24th position in terms of IE, with IE/PE of 17.2hPa/183km. These differences between the ranking based on IE or RMSE confirm that RMSE may not be the most appropriate measure of forecast accuracy for fields characterized by strong gradients.

Figure 12 shows the HEPS forecast started on the 25th of December (t+60h). For this forecast range, HEPS member 45 had the lowest RMSE and the second lowest IE (0.6Pa/38km, compared with 23hPa/904km for the T_L319L60 forecast, see Table 1c).

Figures 13 shows the IE/PE and the RMSE statistics for all EPS and HEPS forecasts started from the 19th (t+180h) to the 25th (t+36h) of December. Figure 13a shows that for forecast ranges longer than 96h none of the EPS members had IE/PE smaller than 10hPa/300km and that only at most eight members had intensity/position errors smaller than 20hPa/600km. These numbers were higher for shorter forecast ranges up to t+60h but they decreased for the t+36h forecast. A possible reason for this poor 36-hour prediction is that the EPS initial perturbations are optimized to generate the proper spread among the ensemble members after 2 days of integration (see section 1). Figure 13b shows the number of EPS members with RMSE smaller than 5 and 10hPa for all forecast issued from the 20th (t+180h) to the 26th (t+36h) of December. The number of EPS members with RMSE smaller than 10hPa steadily increased with forecast time, but only up to six EPS members had an RMSE smaller than 5hPa (note that the RMSE of the T_L319L60 model was lower than 5hPa only for the 156h forecast range, and that the RMSE of the EPS control was always larger than 5hPa). The HEPS had a slightly larger number of ensemble members with low intensity/position errors (Fig. 13a), but it had fewer members with low RMSE (Fig. 13b).

Table 4 lists in more details the number of EPS and HEPS forecasts issued on the 22nd (t+132h) and on the 25th (t+60h) of December with IE/PE within predefined intervals. Table 4 shows that the number of EPS members with IE/PE smaller than 10hPa/300km increases from zero to three between the t+132h and the t+60h. At both these ranges, the HEPS and the EPS had a similar number of forecasts with low IE/PE.

6. Conclusion

From December 1992 to December 1996, the European Centre for Medium-Range Weather Forecasts (ECMWF) had been running operationally the Ensemble Prediction System (EPS) with a 33 members with spectral triangular truncation T63 and 19 vertical levels (T63L19). In December 1996, the EPS resolution was enhanced to T_L159L31 (the subscript 'L' stands for linear grid) and the ensemble size to 51 members. In October 1999 the number of vertical levels was enhanced to 40. The EPS resolution was further increased to T_L255L40 on 21st of November 2000, with initial conditions generated from a high-resolution analysis (T_L511L60), has been tested at ECMWF.

This work discussed the performance of the operational EPS and of the high-resolution HEPS during two periods of December 1999 characterized by intense storms over Europe. Forecast verification focused on mean-sea-level-pressure (MSLP). The quality of single deterministic forecasts has been assessed by computing the intensity and position error in the prediction of the MSLP minimum value and by computing the root-mean-square error (RMSE) inside a verification area centered on the cyclone position. Ensemble performance had been assessed by statistics based on the number of members with low intensity, position and root-mean-square error. Due to the limited number of cases investigated, the verification of probabilistic products had not been considered. A proper evaluation of the impact of resolution on ensemble probabilistic forecasts for a 3-month period is under way and will be the subject of a separate paper.

The EPS proved to be particularly helpful in cases of large inconsistency between deterministic T_L319L60 forecasts issued on successive days. In fact, EPS forecasts started on successive days confirmed and refined earlier ensemble forecasts in a more consistent way than successive deterministic T_L319L60 forecasts.

The EPS performed differently during the three cases. It was very successful in predicting the Danish storm, with EPS forecasts started on subsequent days consistently increasing the probability of occurrence and with many EPS members correctly predicting the intensity and the position of the storm. For this case characterized by a large-scale cyclone, the EPS gave some indications of the possibility of a severe storm affecting Denmark 132-hours before the event. The prediction was less accurate during the two French storms, with fewer EPS members correctly predicting the intensity and the position of the MSLP minimum value. This was particularly true for the first storm, which was characterized by a very small-scale vortex moving very rapidly across Europe. During the two French storms, the EPS provided forecasters with some indications of the chance of an intense storm 72- to 48-hours before the event. By contrast, the ECMWF deterministic T_L319L60 model did not give any useful indications especially in the case of the second French storm.

The impact of horizontal resolution on the ensemble performance was also discussed. Results indicated that the high-resolution ensemble HEPS, based on T_L255L40 integration with initial conditions defined from the unperturbed T_L511L60 analysis, was better capable to correctly predict the intensity of severe storms. This positive impact was evident in the case of the Danish storm, was still positive but less detectable in the case of the first French storm but was neutral in the case of the second French storm. Although strong and statistically significant conclusions on the impact of resolution on ensemble performance cannot be drawn from these results, the indications were that high resolution is required to simulate small-scale features. The overall performance of the EPS and the HEPS system on a larger data set and using a larger set of verification measure will be the subject of a future study.

One of the difficult aspects of ensemble prediction is how to summarize the forecast information contained in the ensemble without oversimplifying it. Results have indicated that the ensemble-mean, which can be considered as the most immediate way to condense the ensemble of forecasts, may not be a useful forecast product in cases of extreme events. By contrast, MSLP stamp-maps showing all EPS members can provide the forecasters with indications of possible extreme weather events.

Longer advance warnings of severe weather events are increasingly requested to improve public safety and reduce economic damages (*Anthes et al* 2001). The ECMWF Ensemble Prediction System is a practical tool designed to assist users to issue weather predictions. The latest increase in resolution of the EPS implemented in November 2001 is part of the ECMWF continuous efforts to improve forecast quality and to develop a forecasting system of severe weather events such as the winter storms that caused casualties and huge damages to some European Countries in December 1999.

Acknowledgements

Martin Leutbecher is thanked for providing the software used to identify local minimum values of mean-sea-level-pressure. The authors are also thankful to an anonymous referee whose comments helped to improve the manuscript.

References

Anthes, R., Fellows, J., Hooke, B., & McPherson, R., 2001: AMS/UCAR outreach to the Bush Administration and the 107th Congress. *Bull. Amer. Meteorol. Soc.*, **82**, 987-990.

Barkmeijer, J., Buizza, R., & Palmer, T. N., 1999: 3D-Var Hessian singular vectors and their potential use in the ECMWF Ensemble Prediction System. *Q. J. R. Meteor. Soc.*, **125**, 2333-2351.

Bell, G. D., Halpert, M. S., Schnell, R. C., Wayne Higgins, R., Lawrimore, J., Kousky, V. E., Tinker, R., Thiaw, W., Chelliah, M., and Artusa, A.: 2000: Climate assesment for 1999. *Bull. Amer. Met. Soc.*, **81**, S1-S50.

Buizza, R. B., & Palmer, T. N., 1995: The singular-vector structure of the atmospheric general circulation. *J. Atmos. Sci.*, **52**, 9, 1434-1456.

————, Petroliagis, T., Palmer, T. N., Barkmeijer, J., Hamrud, M., Hollingsworth, A., Simmons, A., & Wedi, N., 1998: Impact of model resolution and ensemble size on the performance of the ECMWF ensemble prediction system. *Q. J. R. Meteorol. Soc.*, **124**, 1935-1960.

————, Miller, M., & Palmer, T. N., 1999: Stochastic representation of model uncertainties in the ECMWF Ensemble Prediction System. *Q. J. R. Meteorol. Soc.*, **125**, 2887-2908.

Easterling, D. R., Evans, J. L., Groisman, P. Ya., Karl, T. R., Kunkel, K. E., & Ambenje, P., 1999: Observed variability and trends in severe weather climate events: a brief reviw. *Bull. Amer. Meteorol. Soc.*, **81**, 417-425.

Houtekamer, P. L., Lefaivre, L., Derome, J., Ritchie, H., & Mitchell, H. L., 1996: A system simulation approach to ensemble prediction. *Mon. Wea. Rev.*, **124**, 1225-1242.

Kunkel, K. E., Pielke Jr., R. A., & Changnon, S. A., 1999: Temporal fluctuations in weather and climate extremes that cause economic and human health impacts: A review. *Bull. Amer. Meteorol. Soc.*, **80**, 1077-1098.

Molteni, F., Buizza, R., Palmer, T. N., & Petroliagis, T., 1996: The ECMWF Ensemble Prediction System: methodology and validation. *Q. J. R. Meteorol. Soc.*, **122**, 73-119.

Palmer, T. N., Molteni, F., Mureau, R., Buizza, R., Chapelet, P, & Tribbia, J., 1993: Ensemble Prediction. *Proc. ECMWF Seminar (1992)*, ECMWF, Shinfield Park, Reading RG2-9AX, UK.

Pielke, R. A., Jr., et al., 1997: Workshop on the Social and Economic Impacts of Weather, April 2-4. Available at http://www.esig.ucar.edu/socasp/weather1.

Teixeira, J., 1999: The impact of increased boundary layer vertical resolution on the ECMWF forecasting system. *ECMWF Research Department Technical Memorandum No. 268*, February 1999, ECMWF, Shinfield Park, Reading RG2-9AX, UK, 55 pp.

Toth, Z., & Kalnay, E., 1993: Ensemble forecasting at NMC: the generation of perturbations. *Bull. Am. Meteorol. Soc.*, **74**, 2317-2330.

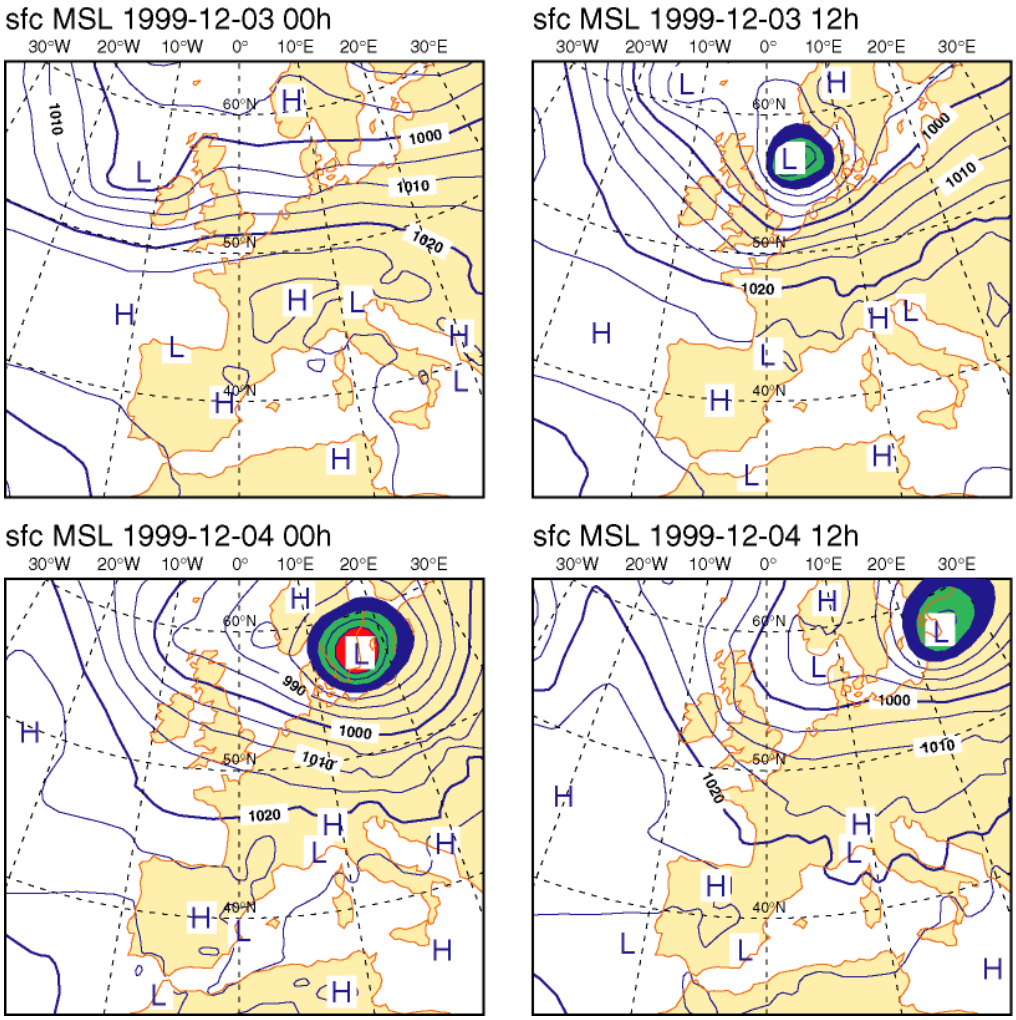

Figure 1. Danish storm. (a) MSLP analysis at 00 UTC on the 3rd of December 1999. (b) as (a) but at 12 UTC on the 3rd. (c) as (a) but at 00 UTC on the 4th. (d) as (a) but at 12 UTC on the 4th. Contour interval is 5hPa, with shading for values below 980hPa.

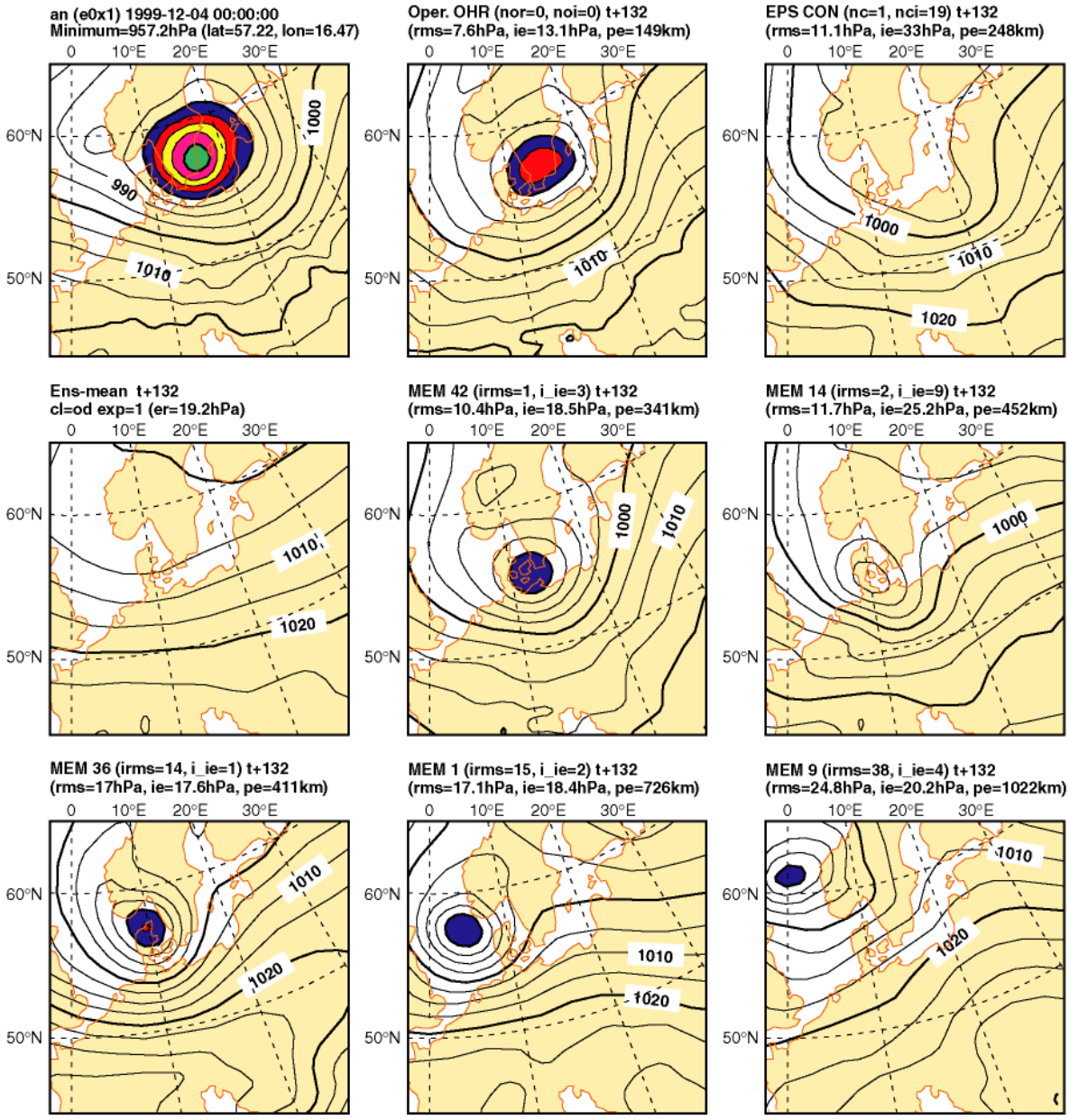

Figure 2. Danish storm. (a) MSLP analysis at 00 UTC on the 4th of December 1999 and (b-l) t+132h T_L319L60 and EPS forecasts started at 12 UTC on the 28th of November. (b) T_L319L60 forecast; (c) EPS control forecast; (d) EPS ensemble-mean forecast; (e-f) the two EPS members with the lowest RMSE; (g-i) the three EPS members with the smallest IE. In panels (b) and (c), *nor* and *noi* in the title indicate the number of EPS perturbed members with RMSE smaller than the T_L319L60 and the EPS control forecast. For all single forecast, the RMSE, IE and PE is reported in the panel title; for each ensemble perturbed member, the ranking position with respect to RMSE (*irms*) and IE (*iie*) (1 is given to the forecast with the smallest error) is also reported. Contour interval is 5hPa, with shading for values below 980hPa.

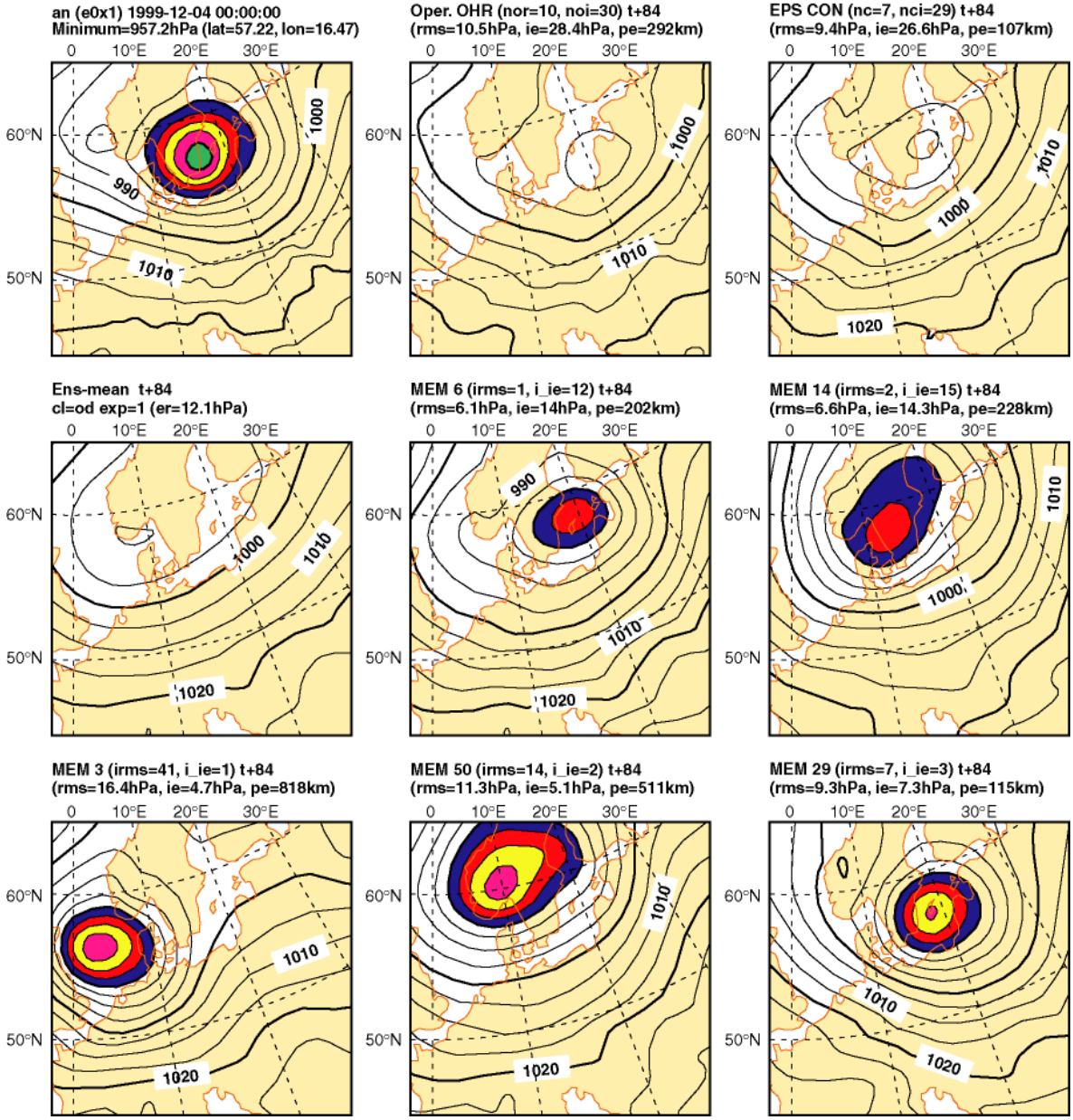

Figure 3. Danish storm. As Fig. 2 but showing t+84h T_L319L60 and EPS forecasts started at 12 UTC on the 30th of November.

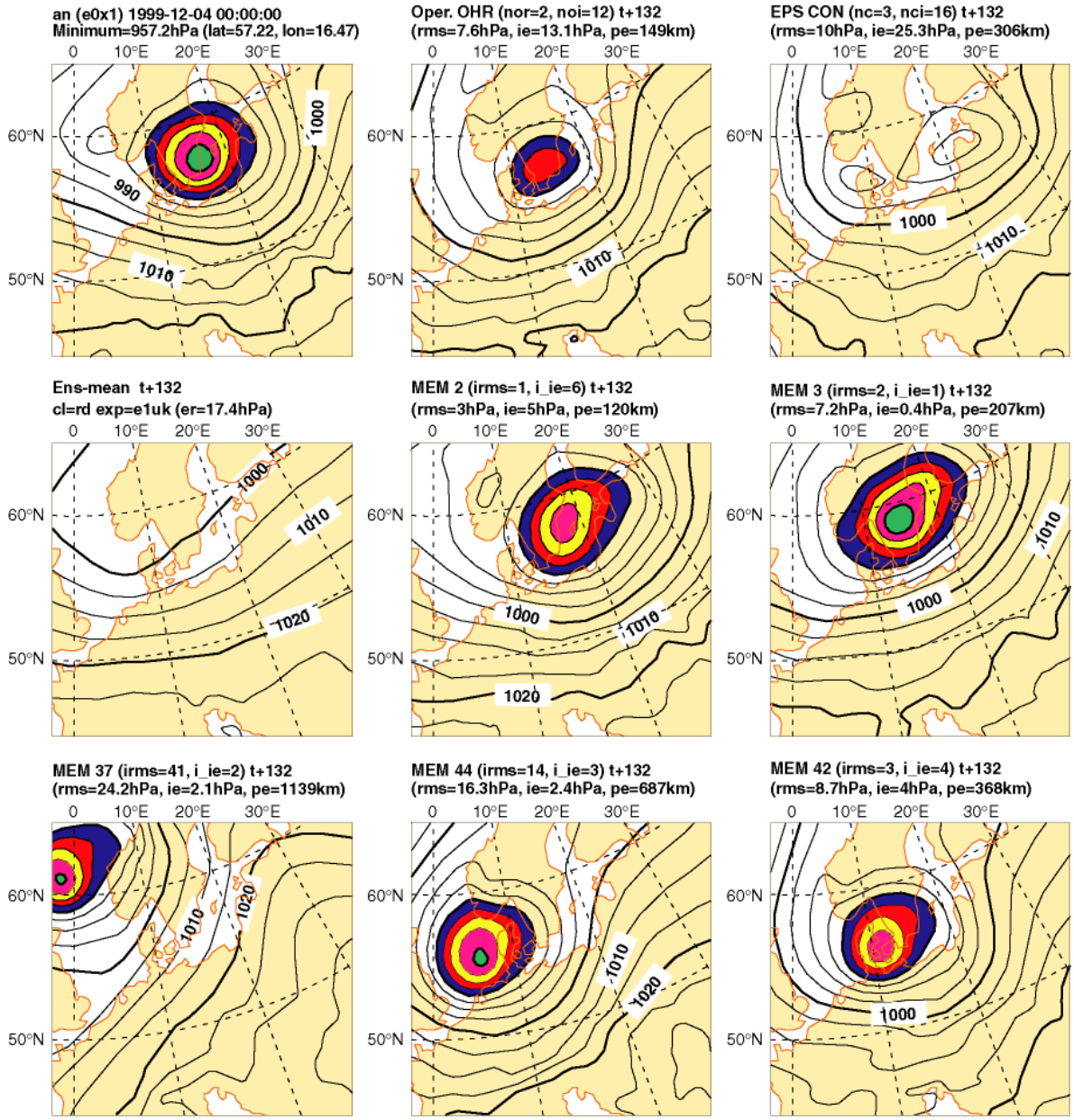

Figure 4. Danish storm. As Fig. 2 but showing HEPS forecasts.

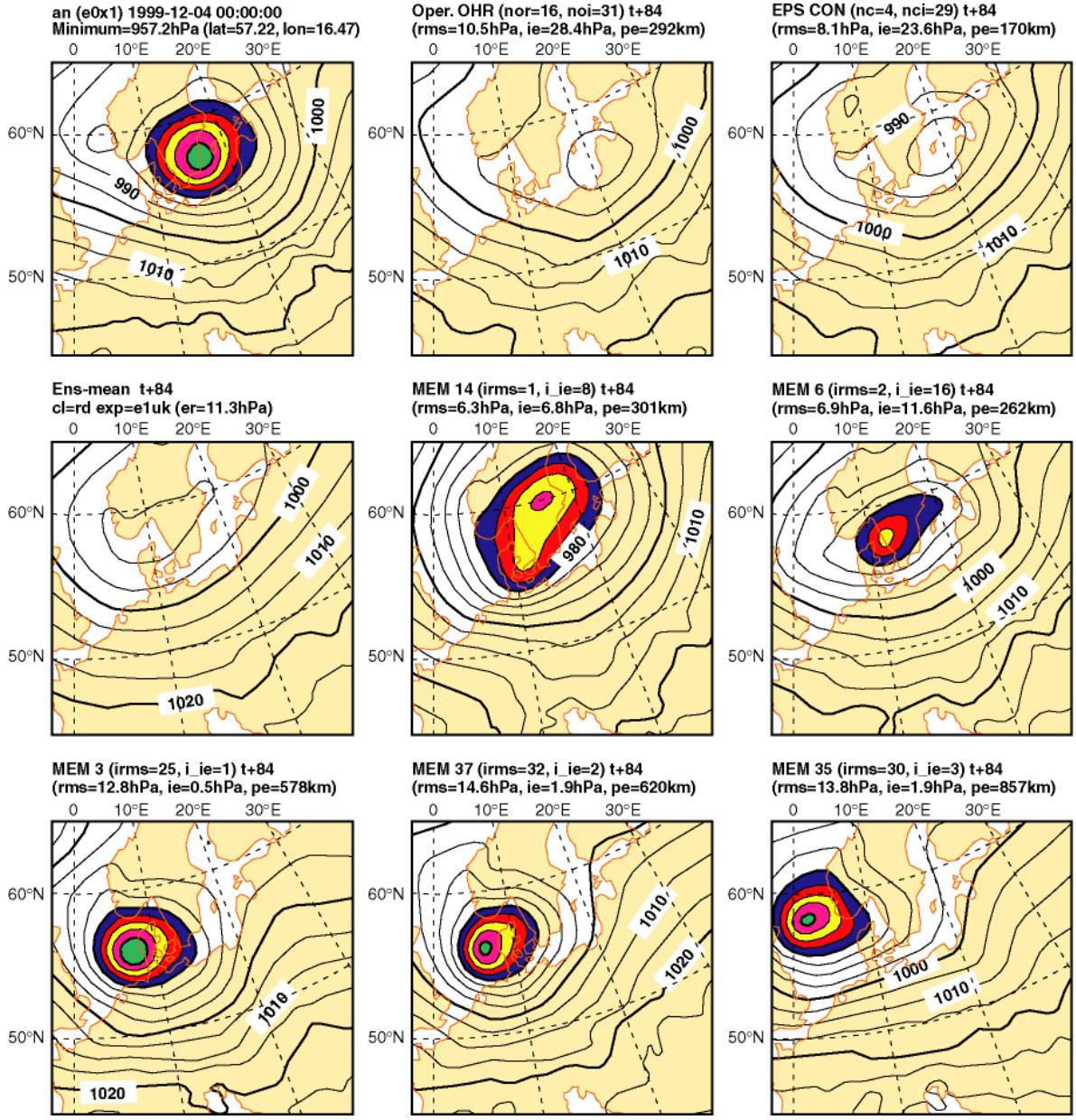

Figure 5. Danish storm. As Fig. 3 but showing HEPS forecasts.

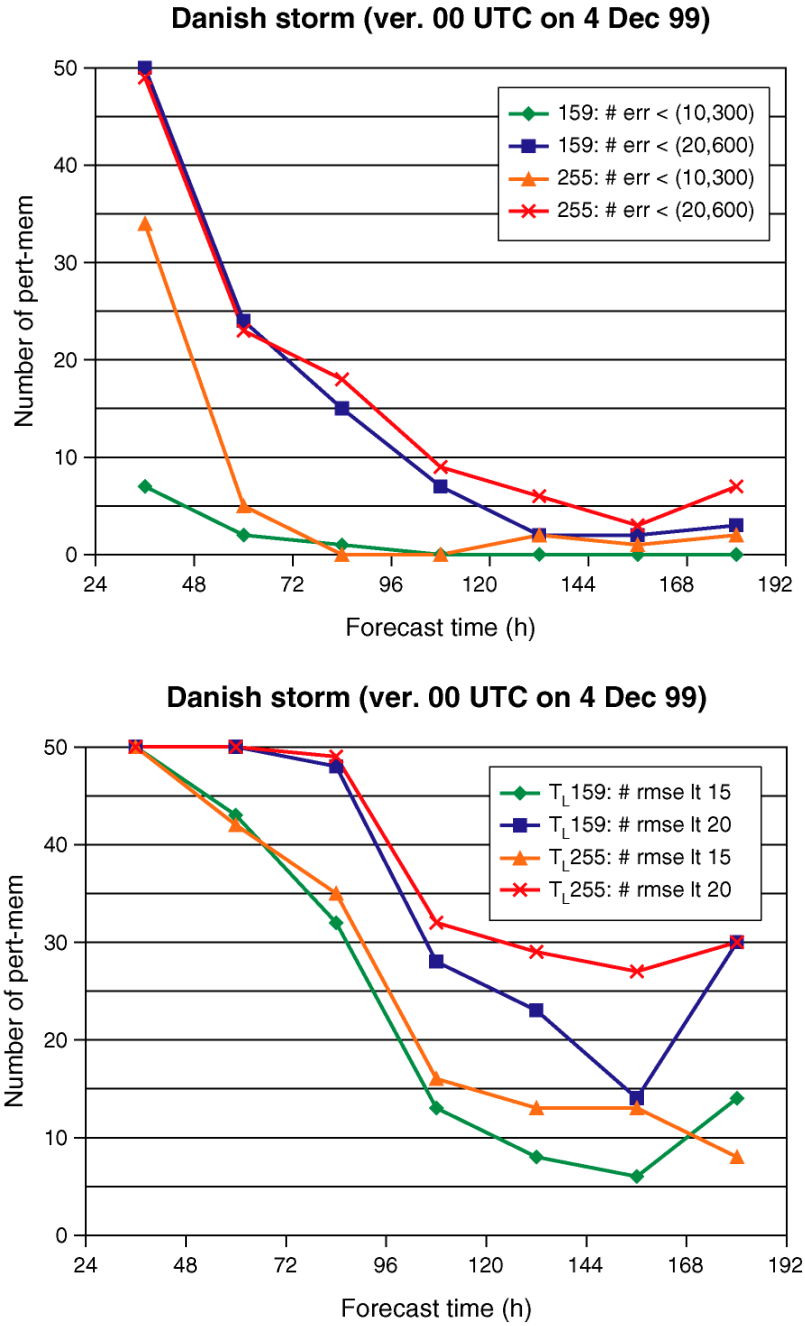

Figure 6. Danish storm, MSLP forecasts verified at 00 UTC on the 4th of December 1999. (a) Number of EPS perturbed members with IE/PE≤10hPa/300km (dashed line with diamonds) and with IE/PE≤20hPa/600km (dotted line with squares), number of HEPS perturbed members with IE/PE≤10hPa/300km (dotted line with triangles) and with IE/PE≤20hPa/600km (solid line with crosses). (b) Number of EPS perturbed members with RMSE≤15hPa (dashed line with diamonds) and RMSE≤20hPa (dotted line with squares) and number of HEPS with RMSE≤15hPa (dotted line with triangles) and RMSE≤20hPa (solid line with crosses).

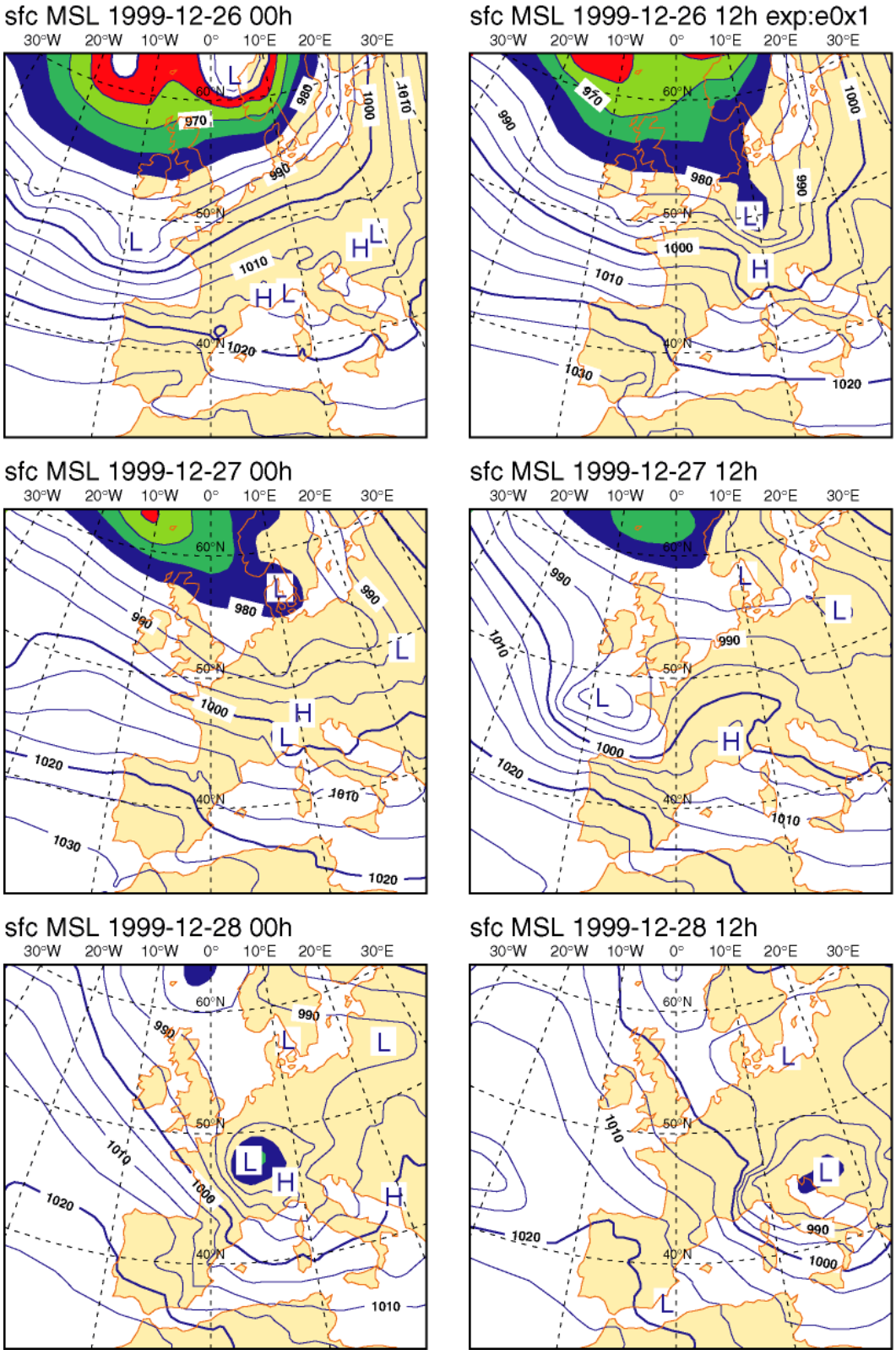

Figure 7. First French storm. (a) MSLP analysis at 00 UTC on the 26th of December 1999, (b) as (a) but at 12 UTC on the 26th, (c) as (a) but at 00 UTC on the 27th, (d) as (a) but at 12 UTC on the 27th, (e): as (a) but at 00 UTC on the 28th, (f) as (a) but at 12 UTC on the 28th. Contour interval is 5hPa, with shading for values below 980hPa.

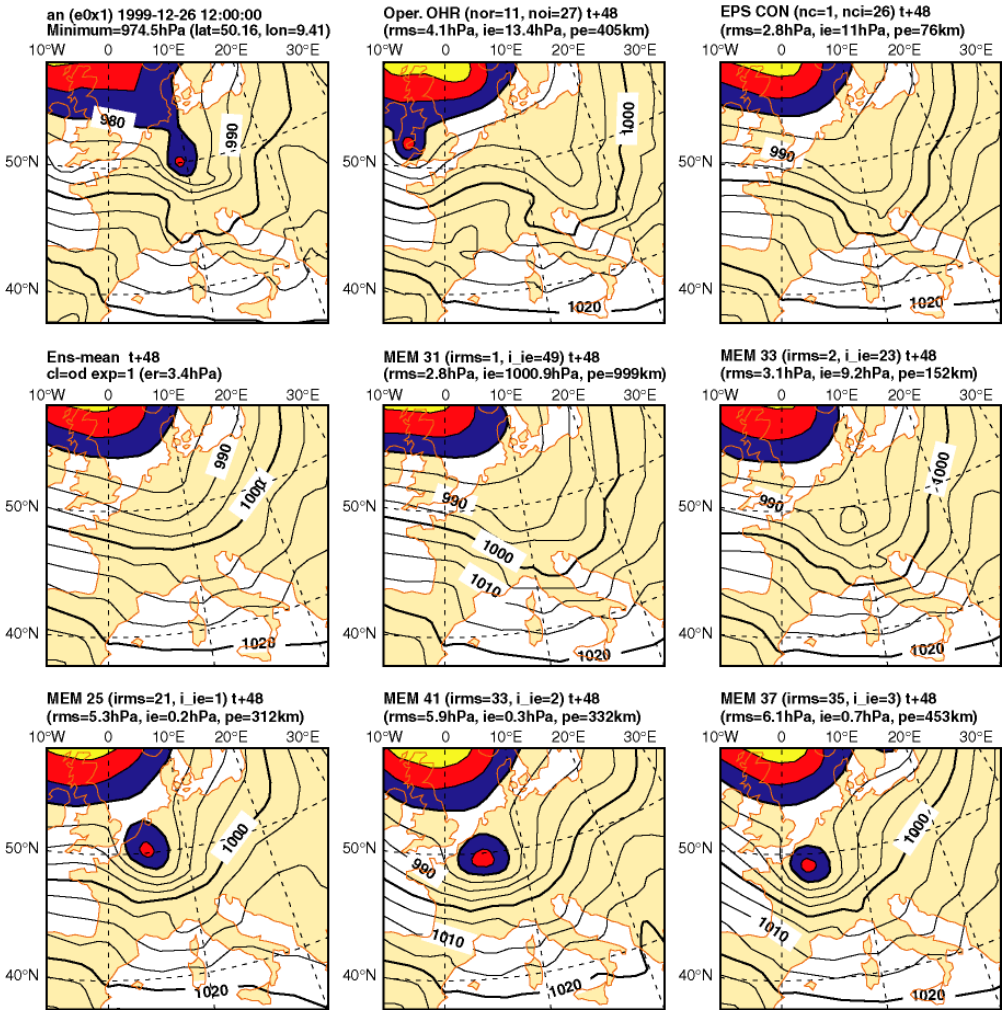

Figure 8. First French storm. (a) MSLP analysis at 12 UTC on the 26th of December 1999 and (b-i) t+48h T_L319L60 and EPS forecasts started at 12 UTC on the 24th of December. (b) T_L319L60 forecast; (c) EPS control forecast; (d) EPS ensemble-mean forecast; (e-f) the two EPS members with the lowest RMSE; (g-i) the three EPS members with the smallest IE. In panels (b) and (c), *nor* and *noi* in the title indicate the number of EPS perturbed members with RMSE smaller than the T_L319L60 and the EPS control forecast. For all single forecast, the RMSE, IE and PE is reported in the panel title. For all single forecast, the RMSE, IE and PE is reported in the panel title; for each ensemble perturbed member, the ranking position with respect to RMSE (*irms*) and IE (*iie*) (1 is given to the forecast with the smallest error) is also reported. Contour interval is 5hPa, with shading for values below 980hPa.

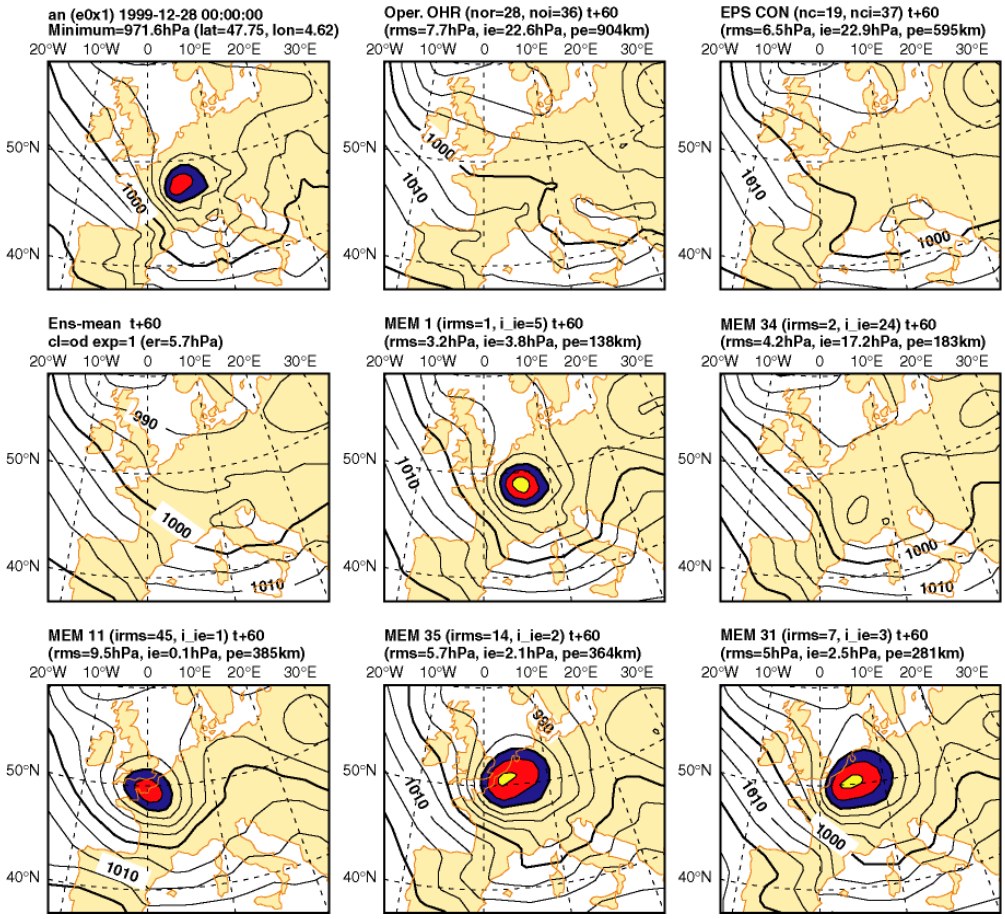

Figure 9. Second French storm. (a) MSLP analysis at 00 UTC on the 28th of December 1999 and (b-i) t+60h T_L319L60 and EPS forecasts started at 12 UTC on the 25th of December. (b) T_L319L60 forecast; (c) EPS control forecast; (d) EPS ensemble-mean forecast; (e-f) the two EPS members with the lowest RMSE; (g-i) the three EPS members with the smallest IE. In panels (b) and (c), *nor* and *noi* in the title indicate the number of EPS perturbed members with RMSE smaller than the T_L319L60 and the EPS control forecast. For all single forecast, the RMSE, IE and PE is reported in the panel title. For all single forecast, the RMSE, IE and PE is reported in the panel title; for each ensemble perturbed member, the ranking position with respect to RMSE (*irms*) and IE (*iie*) (1 is given to the forecast with the smallest error) is also reported. Contour interval is 5hPa, with shading for values below 980hPa.

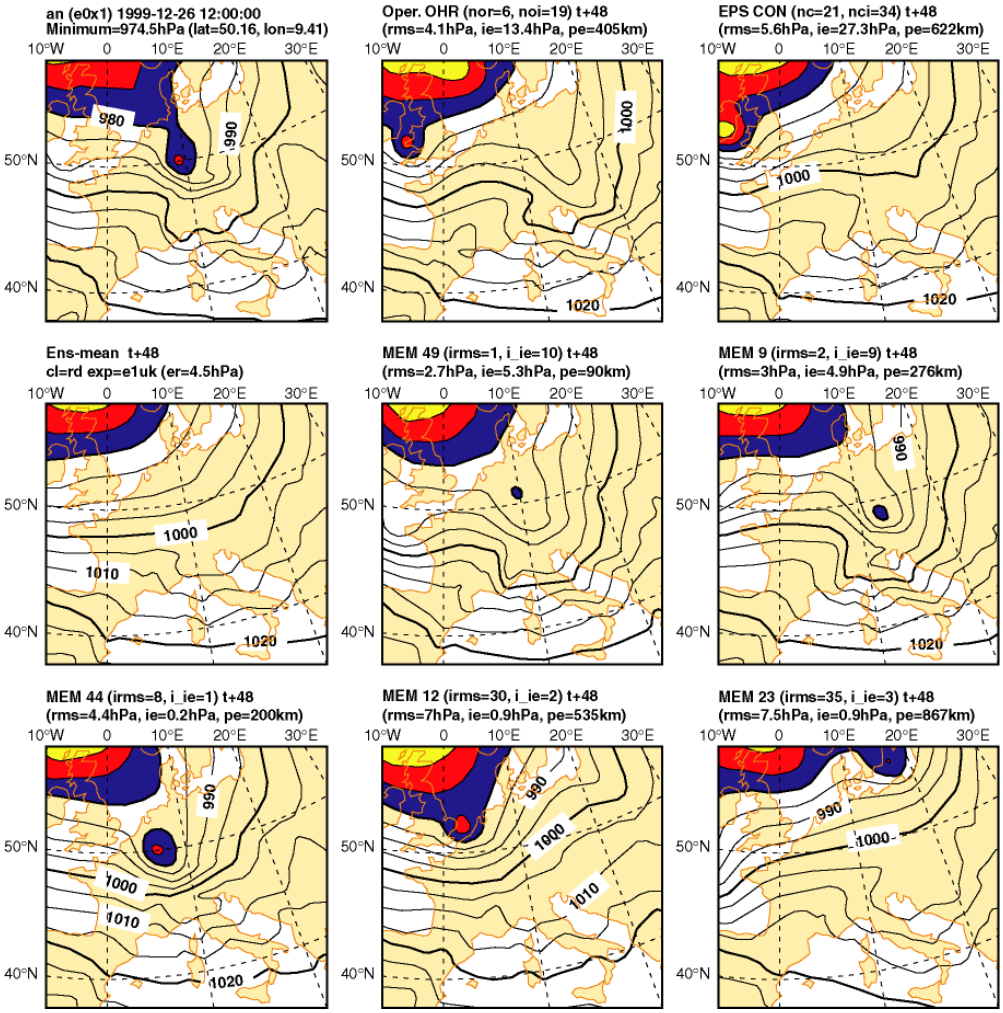

Figure 10. First French storm. As Fig. 8 but showing HEPS forecasts.

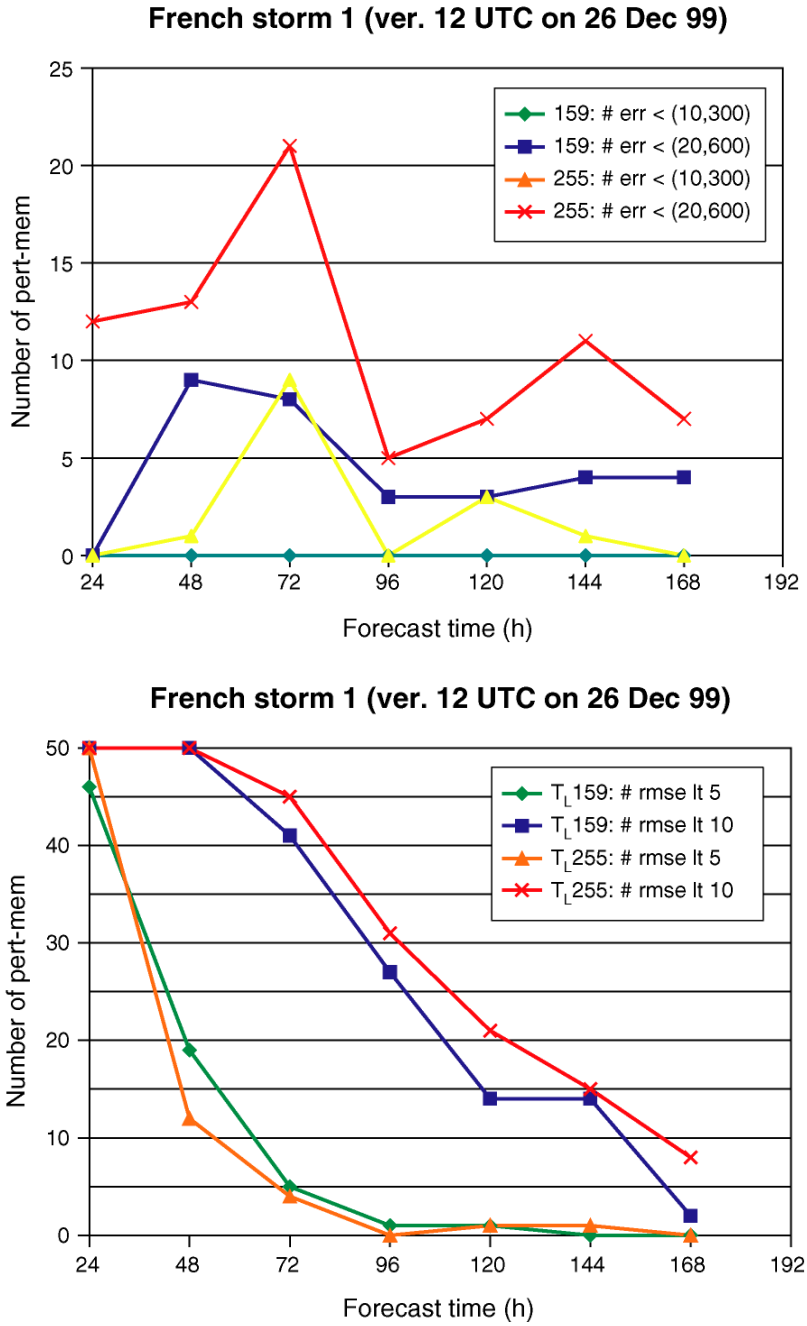

Figure 11. First French storm forecasts verified at 12 UTC on the 26th of December 1999. (a) Number of EPS perturbed members with IE/PE≤10hPa/300km (dashed line with diamonds) and with IE/PE≤20hPa/600km (dotted line with squares), number of HEPS perturbed members with IE/PE≤10hPa/300km (dotted line with triangles) and with IE/PE≤20hPa/600km (solid line with crosses). (b) Number of EPS perturbed members with RMSE≤15hPa (dashed line with diamonds) and RMSE≤20hPa (dotted line with squares) and number of HEPS with RMSE≤15hPa (dotted line with triangles) and RMSE≤20hPa (solid line with crosses).

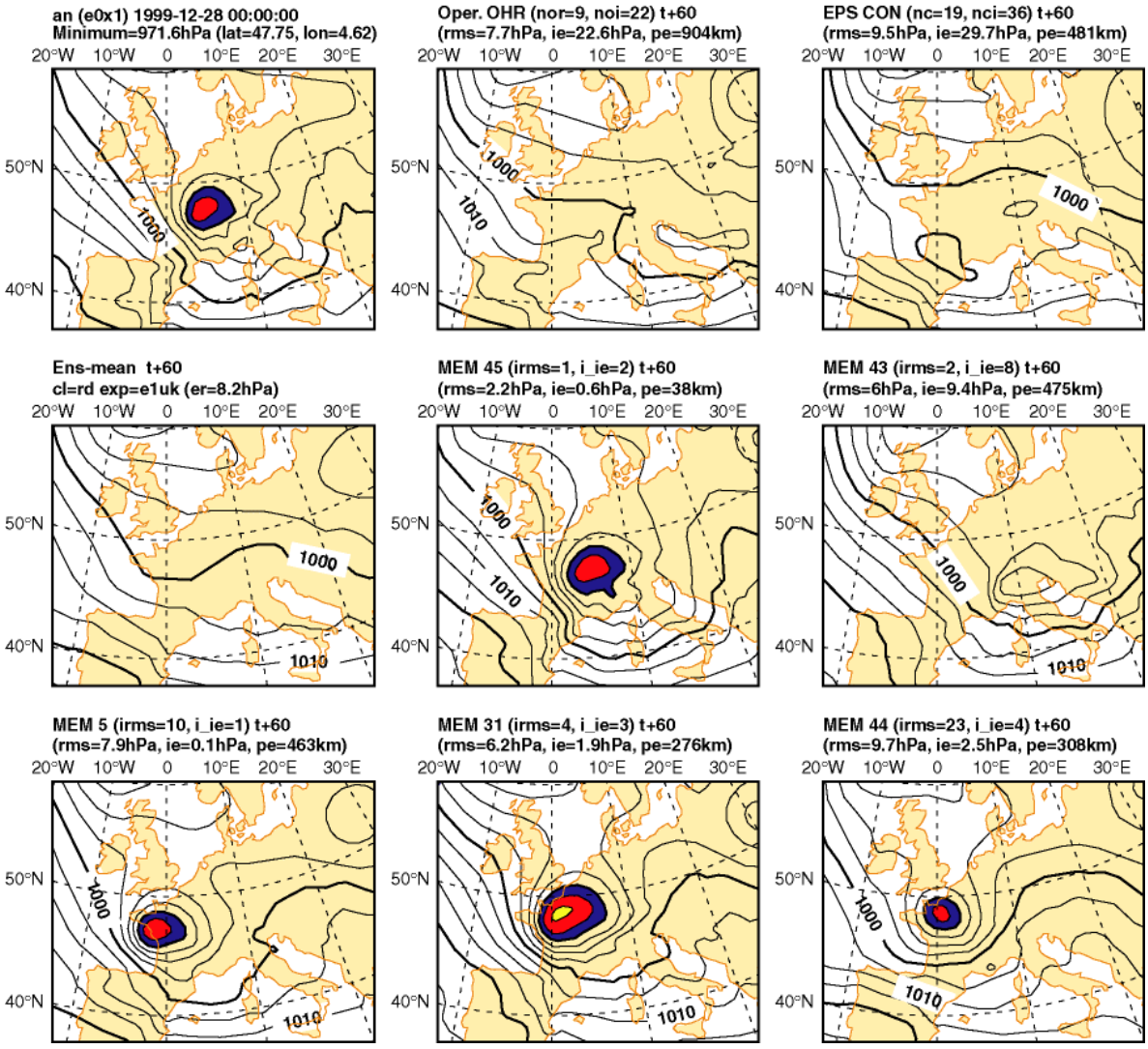

Figure 12. Second French storm verified at 00 UTC on the 28th of December 1999. As Fig. 9 but showing the HEPS forecasts.

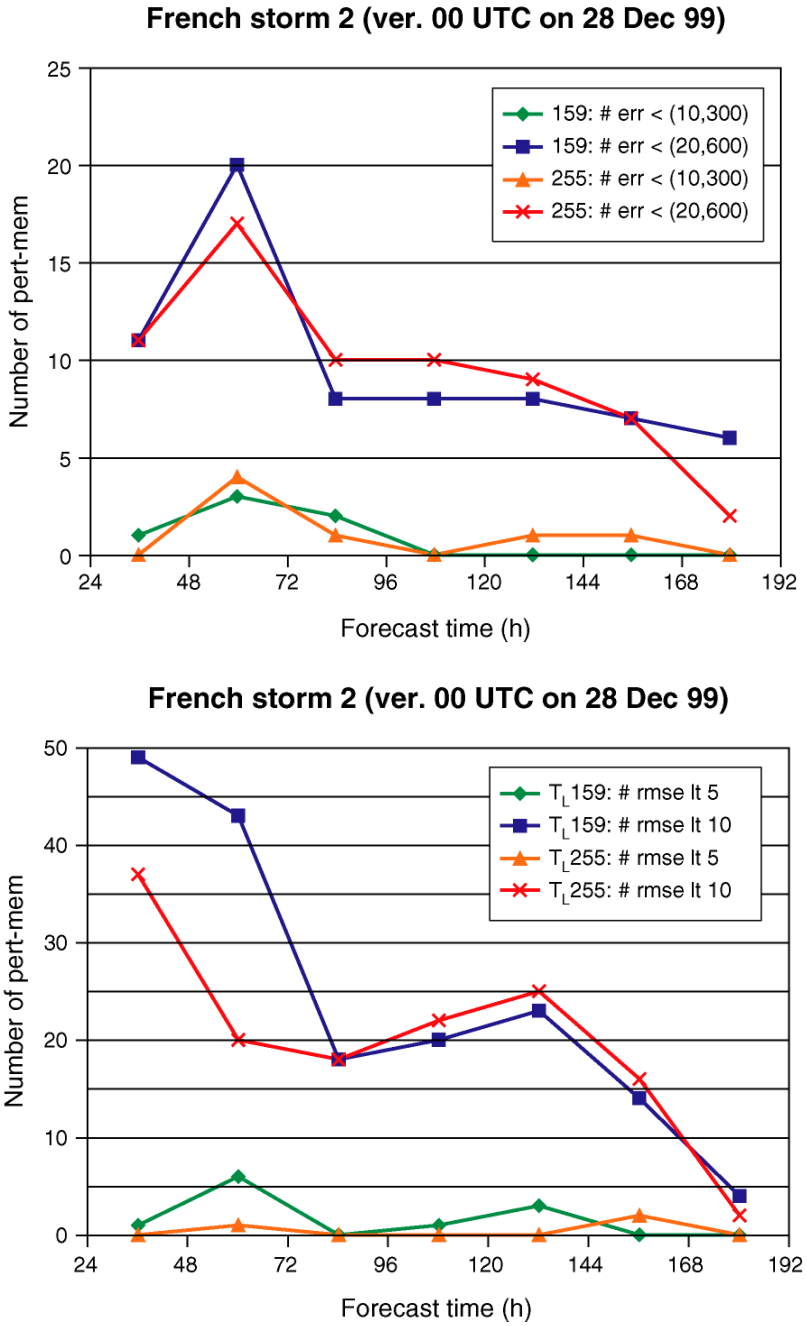

Figure 13. Second French storm forecasts verified at 00 UTC on the 28th of December. As Fig. 11.

Danish Storm (ver. 00 UTC on 4 December 1999)					
Initial date	Forecast time (h)	Intensity error (hPa)		Position error (km)	
		T_L319L60	EPS control	T_L319L60	EPS control
26 Nov	T+180h	24.7	15.8	133	348
27 Nov	T+156h	70.3	30.1	1169	739
28 Nov	T+132h	13.1	33.1	149	249
29 Nov	T+108h	36.1	35.6	394	140
30 Nov	T+84h	28.4	26.7	292	107
1 Dec	T+60h	4.6	9.3	141	111
2 Dec	T+36h	1.3	4.0	81	251

Table 1a.

French Storm (ver. 12 UTC on 26 December 1999)					
Initial date	Forecast time (h)	Intensity error (hPa)		Position error (km)	
		T_L 319L60	EPS control	T_L 319L60	EPS control
19 Dec	T+168h	25.9	35.3	825	231
20 Dec	T+144h	43.7	---	636	---
21 Dec	T+120h	---	---	---	---
22 Dec	T+96h	19.1	5.1	225	507
23 Dec	T+72h	1.3	2.0	366	81
24 Dec	T+48h	13.5	11.1	406	77
25 Dec	T+24h	2.4	3.6	175	128

Table 1b.

French Storm 2 (ver. 00 UTC on 28 December 1999)					
Initial date	Forecast time (h)	Intensity error (hPa)		Position error (km)	
		T_L319L60	EPS control	T_L319L60	EPS control
20 Dec	T+180h	28.3	25.0	1151	751
21 Dec	T+156h	4.3	33.0	169	654
22 Dec	T+132h	14.7	11.8	666	833
23 Dec	T+108h	15.1	18.5	472	134
24 Dec	T+84h	32.2	29.5	471	795
25 Dec	T+60h	22.7	23.0	904	596
26 Dec	T+36h	22.8	23.3	526	623

Table 1c.

Table 1. IE/PE of the T_L319L60 and the EPS T_L159L40 control forecasts for (a) the Danish storm verified at 00UTC on the 4th of December, (b) the French storm verified at 12 UTC on the 26th of December and (c) the French storm 2 verified at 00 UTC on the 28th of December 1999.

Danish Storm (ver. 00 UTC on 4 December 1999)				
28 Nov t+132h	**PE 0-300km**	**PE 300-600km**	**PE 600-900km**	**PE > 900km**
IE 0-10hPa	0 (2)	0 (3)	0 (2)	0 (2)
IE 10-20hPa	0 (0)	2 (1)	1 (3)	0 (0)
IE 20-30hPa	0 (0)	6 (4)	3 (3)	4 (1)
IE > 30hPa	4 (1)	11 (13)	5 (3)	5 (5)

Table 2a

Danish Storm (ver. 00 UTC on 4 December 1999)				
30 Nov t+84h	**PE 0-300km**	**PE 300-600km**	**PE 600-900km**	**PE > 900km**
IE 0-10hPa	1 (0)	2 (4)	1 (6)	0 (0)
IE 10-20hPa	5 (5)	7 (9)	3 (0)	3 (0)
IE 20-30hPa	1 (4)	5 (3)	3 (2)	1 (0)
IE > 30hPa	1 (2)	12 (14)	5 (1)	0 (0)

Table 2b.

Table 2. Danish storm. Number of EPS and HEPS (in brackets) perturbed members with IE and PE included in defined interval, for (a) ensembles started on the 28th of November (t+132h) and (b) on the 30th of November (t+84h).

French Storm (ver. 12UTC on 26 December 1999)				
21 Dec t+120h	**PE 0-300km**	**PE 300-600km**	**PE 600-900km**	**PE > 900km**
IE 0-10hPa	0 (3)	2 (2)	6 (2)	2 (7)
IE 10-20hPa	0 (1)	1 (1)	2 (1)	5 (6)
IE 20-30hPa	0 (0)	1 (1)	0 (2)	0 (1)
IE > 30hPa	0 (0)	0 (1)	19 (14)	0 (4)

Table 3a

French Storm (ver. 12 UTC on 26 December 1999)				
24 Dec t+48h	**PE 0-300km**	**PE 300-600km**	**PE 600-900km**	**PE > 900km**
IE 0-10hPa	0 (1)	6 (6)	16 (5)	3 (2)
IE 10-20hPa	0 (1)	3 (5)	3 (1)	0 (2)
IE 20-30hPa	0 (0)	2 (6)	9 (8)	0 (5)
IE > 30hPa	0 (0)	0 (0)	2 (7)	1 (1)

Table 3b.

Table 3. First French storm. Number of EPS and HEPS (in brackets) perturbed members with IE and PE included in defined interval, for ensembles started (a) on the 21st of December (t+120h) and (b) on the 24th of December (t+48h).

French Storm 2 (ver. 00 UTC on 28 December 1999)				
22 Dec t+132h	**PE 0-300km**	**PE 300-600km**	**PE 600-900km**	**PE > 900km**
IE 0-10hPa	0 (1)	0 (1)	3 (1)	4 (3)
IE 10-20hPa	4 (0)	4 (7)	7 (5)	5 (1)
IE 20-30hPa	0 (0)	1 (11)	8 (9)	2 (2)
IE > 30hPa	0 (0)	4 (2)	5 (3)	1 (3)

Table 4a

French Storm 2 (ver. 00 UTC on 28 December 1999)				
25 Dec t+60h	**PE 0-300km**	**PE 300-600km**	**PE 600-900km**	**PE > 900km**
IE 0-10hPa	3 (4)	5 (4)	0 (0)	1 (1)
IE 10-20hPa	6 (1)	6 (4)	8 (1)	3 (3)
IE 20-30hPa	1 (1)	8 (8)	4 (7)	0 (3)
IE > 30hPa	0 (1)	0 (10)	5 (3)	1 (0)

Table 4b.

Table 4. Second French storm. Number of EPS and HEPS (in brackets) perturbed members with IE and PE included in defined interval, for ensembles started (a) on the 22nd of December (t+132h) and (b) on the 25th of December (t+60h).